Asian Journal of Atmospheric Environment
Vol. 10-1, pp. 1-12, March 2016
doi: http://dx.doi.org/10.5572/ajae.2016.10.1.001

ISSN (Online) 2287-1160
ISSN (Print) 1976-6912

On-line Measurement of the Surface Area Concentration of Aerosols in Yokohama, Japan, using the Diffusion Charging Method

Kazuki Hatoya, Tomoaki Okuda*, Koji Funato[1)] and Kozo Inoue[1)]

Department of Applied Chemistry, Faculty of Science and Technology, Keio University, 3-14-1 Hiyoshi, Kohoku-ku, Yokohama 223-8522, Japan
[1)]Tokyo Dylec Corp., Naito-cho Bldg., 1 Naito-machi, Shinjuku-ku, Tokyo 160-0014, Japan

*Corresponding author. Tel: +81-45-566-1578, E-mail: okuda@applc.keio.ac.jp

ABSTRACT

Numerous researchers have proposed that surface area is a more appropriate indicator than mass for evaluating pulmonary inflammatory responses caused by exposure to fine and ultrafine particles. In this study, measurements of surface area concentrations of aerosols were conducted in Yokohama, Japan, using the diffusion charging method. $PM_{2.5}$ mass concentration and black carbon concentration in $PM_{2.5}$ were also measured. The 24-hour continuous measurement campaigns were conducted 39 times from March to November, 2014. The surface area concentration was more closely correlated with the black carbon concentration than with the $PM_{2.5}$ mass concentration. It is considered that the abundance of black carbon particles significantly affects the surface area concentration of $PM_{2.5}$. The strength of the correlation between the surface area and black carbon concentrations varied considerably among the measurement campaigns. A relatively weaker afternoon correlation was observed compared with the other time zones (morning, evening, and night). We consider that these phenomena are due to the transportation/formation of the particles other than black carbon that affects surface area concentration and/or the variation of the surface condition of the black carbon particles.

Key words: Aethalometer, Black carbon, Diffusion charger, Nanoparticle surface area monitor (NSAM), $PM_{2.5}$

1. INTRODUCTION

In the evaluation of adverse health effects, including inhalation (respiratory tract), ingestion (gastrointestinal tract), dermal (skin), and injection (blood circulation), in response to exposure to manufactured nanomaterials, scientific interest has recently shifted from the mass to the surface area of these materials (Oberdörster *et al*., 2005). In particular, nanoparticles whose diameters are less than 100 nm (ultrafine particles) are considered to have a much stronger toxicity than larger particles (Donaldson *et al*., 1998; Oberdörster *et al*., 1995). Numerous researchers conducting particle exposure experiments on rats or mice have proposed that surface area is a more appropriate indicator than mass for evaluating pulmonary inflammatory responses caused by exposure to manufactured nanomaterials, such as TiO_2, fullerene, and carbon nanotubes (Nakanishi, 2011; Oberdörster *et al*., 2005; Oberdörster *et al*., 2000). The relationship between the surface area of the manufactured nanomaterials and their toxicity has been well presented recently. Similarly, surface area of ambient aerosols can be considered as an index of toxicity because increased surface area may be able to act as a catalyst for specific reactions between particle and cells, and also act as a carrier for co-pollutants such as gases and chemicals (Giechaskiel *et al*., 2009; Oberdörster, 2001).

In contrast, mass concentration is currently used as an index of toxicity when adverse health effects caused by exposure to ambient aerosols are discussed since enormous number of previous studies have presented that the mass concentrations of particulate matter is significantly correlated with human respiratory diseases, cardiovascular diseases, and even mortality. For example, the guideline values for mass concentrations of $PM_{2.5}$ (particulate matter in which 50% of the particles have an aerodynamic diameter less than 2.5 μm) prescribed by WHO (2005) are 10 $\mu g/m^3$ (annual mean) and 25 $\mu g/m^3$ (24-hour mean). Measurements of $PM_{2.5}$ mass concentration, which are conducted extensively by many research institutions and administrative organizations, as well as measurements of $PM_{2.5}$ surface area concentration (given aerosol surface area values

per unit volume of air) are needed for more detailed understanding of the adverse health effects caused by $PM_{2.5}$. One of the main reasons that mass concentrations of atmospheric aerosol particles (e.g., $PM_{2.5}$ and PM_{10}) have been measured more extensively than surface area concentrations is that there are more reliable and widely used methods for continuous measurements of mass concentrations. For instance, the mass concentrations of the particles can be measured automatically using beta-attenuation, light scattering, and tapered element oscillating microbalance methods. In contrast, the surface area measurements of ambient aerosols are considered challenging, and scientific progress on these measurements has been limited thus far.

The most common method used for measuring the specific surface area of particles (given surface area values per unit mass), particularly in the field of material science, is the Brunauer-Emmett-Teller (BET) method (Brunauer *et al*., 1938). The relationship between the specific surface area of manufactured nanomaterials and toxicity caused by exposure to these materials has been discussed on the basis of specific surface area values measured using the BET method (Nakanishi, 2011; Oberdörster *et al*., 2005; Oberdörster *et al*., 2000). However, specific surface area measured using the BET method usually requires tens of milligrams of particles as a minimum. For example, Nguyen and Ball (2006) used approximately 100 mg of soot samples and Okuda (2013) used approximately 50 mg of powdered samples of atmospheric aerosol reference materials for the measurement of specific surface area. In addition, sampling periods longer than one week are needed for the collection of 100 mg of $PM_{2.5}$ particles using a high-volume air sampler with an air flow rate of 1,000 L/min, assuming that the $PM_{2.5}$ mass concentration is 10 $\mu g/m^3$. The surface area of $PM_{2.5}$ collected on a filter cannot be analyzed directly using the BET method. Thus, for specific surface area measurement of ambient aerosols using the BET method, samples have to be collected with a cyclone system (Okuda *et al*., 2015; Rule *et al*., 2010), without the use of filters, which are widely used for routine chemical analyses of ambient aerosols.

Consequently, other surface area measurement methods that have a much higher time resolution than the BET method are needed for practical and continuous measurement of ambient aerosol surface area. Several surface area measurement methods have been investigated (Bau *et al*., 2010; Gäggeler *et al*., 1989). In this study, the diffusion charging (DC) method (Heitbrink *et al*., 2009; Jung and Kittelson, 2005) was used to measure the $PM_{2.5}$ surface area concentration. The DC method is superior to the BET method with respect to the capability of on-line measurements with a higher time resolution. In addition, surface area measurements using the DC method do not require complicated sample handling or pretreatment.

A nanoparticle surface area monitor (NSAM) has been developed in order to measure surface area concentration using the DC method (Fissan *et al*., 2007; Shin *et al*., 2007). The NSAM has a mixing chamber, where particles are mixed with positive ions emitted by a corona discharge. Positively charged particles are collected by a conductive filter, and then the current is measured using an electrometer connected to a sensitive amplifier. Excess ions are removed by an ion trap before they reach the conductive filter. The relationship between the electrometer current and the lung deposited surface area (LDSA) concentration of particles can be expressed according to the following equation Eq. (1) (Shin *et al*., 2007):

$$S_A = k \times I \quad (1)$$

where S_A is the LDSA concentration ($\mu m^2/cm^3$), k is the calibration coefficient, and I is the electrometer current (fA).

Eq. (1) is considered to be consistent provided that particle diameter lies within a range between tens of nanometers and approximately 400 nm, i.e., the electrometer current is proportional to the square of the particle diameter within this range, but is proportional to the particle diameter (not the square) at diameters that exceed this range (Kulkarni *et al*., 2011; Jung and Kittelson, 2005; Gäggeler *et al*., 1989). Therefore, when polydisperse ambient aerosols, including $PM_{2.5}$, are measured using the DC method, a properly measurable diameter range of the particles should be noted. However, Whitby (1978) showed that particle sizes ranging from approximately tens of nanometers to 400-500 nm contributed greatly to total surface area concentration of ambient aerosols. Consequently, we consider that surface area concentration of $PM_{2.5}$ can be appropriately measured using the DC method.

Interpretation of the LDSA value measured using NSAM is still open for further discussion. A common understanding about the performance of NSAM would be that the LDSA value measured using NSAM is equivalent to those calculated using particle size distribution of monodisperse aerosols measured by scanning mobility particle sizer (SMPS) (Bau *et al*., 2012; Asbach *et al*., 2009; Shin *et al*., 2007). However, several studies showed that NSAM would underestimate the surface area value of polydisperse aerosols or liquid droplets when compared to the calculated surface area value using SMPS data (Kaminski *et al*., 2013; Leavey *et al*., 2013; Bau *et al*., 2012). Nevertheless, Mokhtar *et al*. (2013) showed that the surface area values of ambient aerosols, which were indeed polydisperse, measured

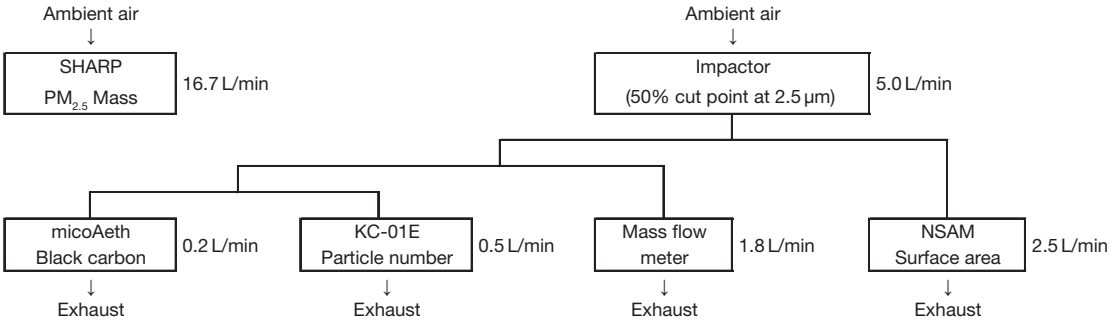

Fig. 1. Schematic of the experimental setup.

using NSAM were equivalent to those calculated using SMPS, under a non-nucleation condition where new particle formation was not active in ambient air. To date, the number of field observation using NSAM was quite limited. Hence, this study will contribute to show a field performance of NSAM for measuring the surface area value of ambient aerosols.

Most of the previous research conducted using the DC method used targeted manufactured nanomaterials (Bau *et al*., 2012; LeBouf *et al*., 2011; Ku, 2010) or diesel exhaust particles, including soot particles (Ntziachristos *et al*., 2007a; Kittelson *et al*., 2005; Ntziachristos *et al*., 2004). In addition, the surface area of ambient aerosols were measured using the DC method in some studies (Albuquerque *et al*., 2012; Ntziachristos *et al*., 2007b; Velasco *et al*., 2004). However, the sampling periods of these field studies were a few weeks at most, and long-term measurements of the surface area of ambient aerosols at one site have seldom been conducted. In this study, the surface area concentration of $PM_{2.5}$ was measured in Yokohama, Japan for a period of nine months. This paper will provide some ideas of what controls the surface area concentration of ambient aerosols in an East Asian urban area.

In general, BC particles are considered to be agglomerates consisting of primary particles whose diameters lie within the range of tens of nanometers, and the sizes of the agglomerates are regarded as hundreds of nanometers (China *et al*., 2014). In other words, BC is likely to have the highest specific surface area among the chemical species constituting $PM_{2.5}$. Hence, the BC concentration may affect the total $PM_{2.5}$ surface area concentration, and thus the BC concentration in $PM_{2.5}$ and the surface area concentration measured on the NSAM were compared in this study.

2. METHODS

The surface area concentration as well as the concentrations of $PM_{2.5}$ mass, number, and black carbon (BC) were measured in this study. A schematic of the experimental setup is shown in Fig. 1. The instruments were operated simultaneously. We focused on $PM_{2.5}$ using an impactor at the inlet of the sampling instruments. The following sections contain brief descriptions of each measurement method and instrument.

2. 1 Surface Area Concentration Measurement

A nanoparticle surface area monitor (NSAM, Model 3550, TSI Inc.) was used to measure surface area concentration using the DC method. The flow rate of the NSAM is 2.5 L/min. The NSAM has a cyclone whose 50% cut-off point is at 1 μm at the inlet, and thus the surface area concentration of $PM_{1.0}$ is actually measured with the NSAM. However, Whitby (1978) showed that total surface area concentration of ambient aerosol particles larger than 1 μm is negligibly small compared with those of particles smaller than 1 μm. Hence, we consider that surface area concentration of $PM_{2.5}$ was measured using the NSAM in this study.

The NSAM calibration constant is determined by running the monodispersed aerosol simultaneously between the SMPS and the NSAM (TSI Inc., 2010). Briefly, the total surface area of the 80 nm NaCl particles determined by the SMPS is then multiplied by the lung deposition efficiency of 80 nm particles as determined by the lung deposition curve for a reference worker reported by ICRP (Vincent, 1999; ICRP, 1994). In this study, we measured the tracheobronchial deposited surface area values by the NSAM, and then converted them into aerosol surface area by dividing by the ICRP deposition efficiency of 80 nm particles.

2. 2 Mass Concentration Measurement

A synchronized hybrid ambient real-time particulate monitor (SHARP Monitor, Model 5030, Thermo Fisher Scientific Inc.) was used for continuous measurement of mass concentration of $PM_{2.5}$. The SHARP is a US

Table 1. Sampling periods for each measurement instrument used in this study.

Measurement metrics	Instruments	Sampling periods (year 2014)	Daily samples
Surface area	NSAM	3rd March - 28th November	39
Mass	SHARP	3rd March - 28th November	39
Number	KC-01E	3rd March - 28th November	39
Black carbon	microAeth	19th June - 28th November	22

EPA (2009) approved $PM_{2.5}$ mass concentration monitor based on the light scattering and beta-attenuation methods. The flow rate of the SHARP is 16.7 L/min.

The specific surface area (given surface area values per mass) of $PM_{2.5}$ in this study is defined as the measurement value of $PM_{2.5}$ surface area concentration divided by the measurement value of $PM_{2.5}$ mass concentration ($(\mu m^2/cm^3) / (\mu g/m^3) = m^2/g$). An increase in the surface area value does not necessarily represent an increase in the abundance of smaller particles; however, an increase in the specific surface area value directly represents an increase in the abundance of smaller particles.

2. 3 Number Concentration Measurement

An optical particle counter (OPC, KC-01E, RION Co., Ltd.) was used for number concentration measurements for ambient aerosol particles. Particles larger than 0.3 μm can be measured with 5 channels (0.3, 0.5, 1.0, 2.0, and 5.0 μm) on the KC-01E. The flow rate of the OPC is 0.5 L/min. The $PM_{2.5}$ number concentration measured using the OPC and the $PM_{2.5}$ surface area concentration measured using the NSAM were compared. Moreover, the surface area concentration can be estimated from number concentration using a calculation based on the assumption that the shape of particles is spherical and measured optical equivalent diameter is considered as geometric diameter. Consequently, the surface area concentrations estimated from measurement values of the OPC and measurements conducted using the NSAM were compared.

2. 4 Black Carbon Concentration Measurement

An aethalometer (microAeth, Model AE51, AethLabs: Cheng and Lin, 2013; Ferrero *et al*., 2011) was used for measuring the BC mass concentration in $PM_{2.5}$. Here, the BC concentration (ng/m^3) is estimated on the basis of the absorption rate of incident light, i.e., visible or near infrared, caused by BC. The wavelength of the incident light used in the microAeth is 880 nm, and the flow rate is 0.2 L/min. Time resolution of BC measurement by AE51 was set at 5 min in this study. Previous paper reported that 24-h average of real-time BC concentration data obtained by AE51 agreed well with the BC concentration obtained from 24-h integrated $PM_{2.5}$ filter deposits (Cai *et al*., 2014).

2. 5 Sampling Site and Periods

The sampling site is located at Keio University Yagami Campus in a residential area of Yokohama, Japan (Okuda *et al*., 2007). The distance between the sampling site and Daisan Keihin Road, which is the nearest expressway to the site and links Tokyo with Yokohama, is about 4 kilometers. In addition, the height of the site from the ground roads is approximately 30 meters. The sampling environment in this study is quite different from that in previous studies where sampling was conducted next to expressways (Albuquerque *et al*., 2012; Ntziachristos *et al*., 2007b).

Continuous measurements were conducted for 24 hours in each experiment, and hourly mean values and daily mean values were obtained. The measurement campaigns were conducted 39 times from March to November, 2014. The sampling periods are divided into three seasons, namely, spring (March to May), summer (June to August), and fall (September to November). The sampling periods differ somewhat depending on the measurement instruments (Table 1).

3. RESULTS AND DISCUSSION

3. 1 Comparison between Mass and Surface Area Concentrations

If temporal variation of $PM_{2.5}$ surface area concentration corresponds to that of the mass concentration at all time periods, measurements of surface area concentration may not be necessary. In order to verify this, the concentrations of mass and surface area were compared. Figs. 2 and 3 show the diurnal variations of mass and surface area concentrations of $PM_{2.5}$, respectively, in each season: (a) spring, (b) summer, (c) fall, and (d) all seasons. Here, we present the ratio (max/min) of values, defined as the ratio of the maximum divided by the minimum hourly mean values. The ratio (max/min) of mass concentration values in each season were (a) 2.1, (b) 2.9, (c) 2.3, and (d) 2.1. Similarly, the ratio (max/min) of surface area concentration values in each season were (a) 1.5, (b) 1.9, (c) 1.3, and (d) 1.4. The

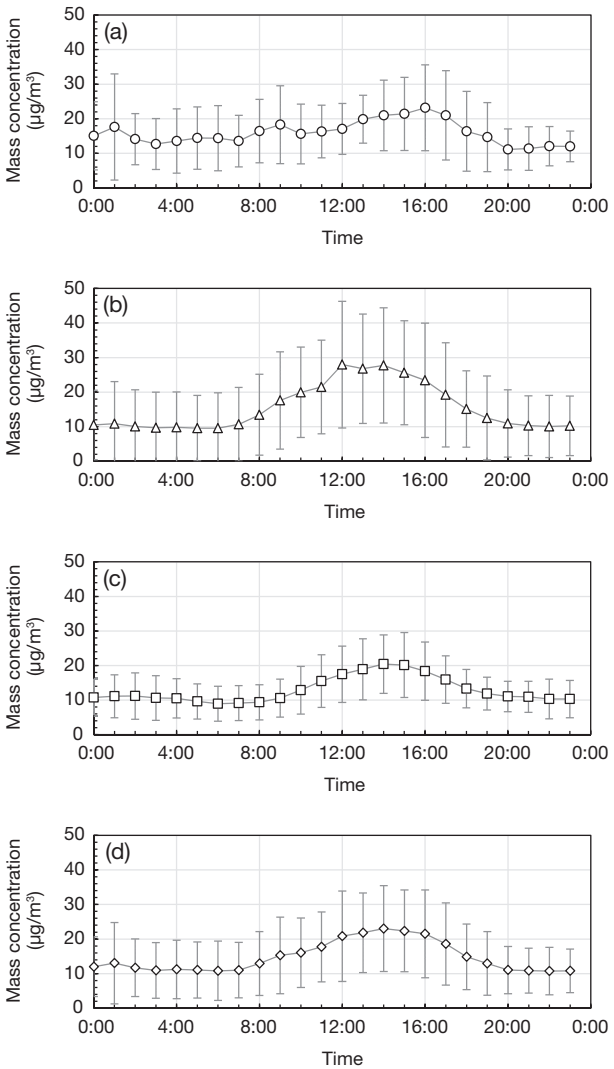

Fig. 2. Diurnal variation of $PM_{2.5}$ mass concentration measured using the SHARP in 24-hour continuous measurements conducted in 2014. (a) Hourly mean values in spring (March to May), (b) summer (June to August), (c) fall (September to November), and (d) across all seasons. Error bars show one standard deviation.

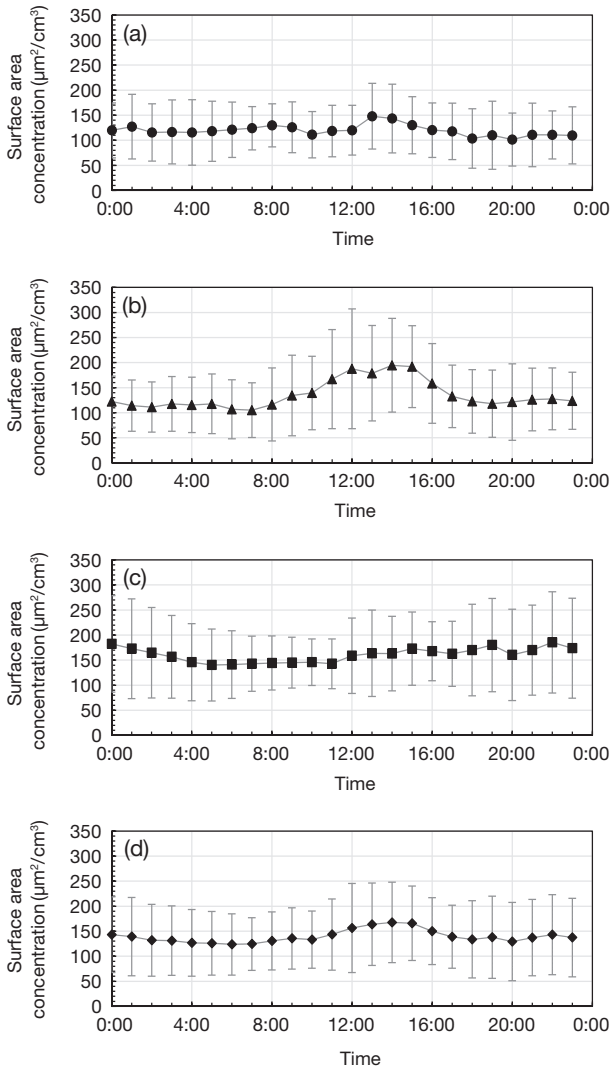

Fig. 3. Diurnal variation of $PM_{2.5}$ surface area concentration measured using the NSAM in 24-hour continuous measurements conducted in 2014. (a) Hourly mean values in spring (March to May), (b) summer (June to August), (c) fall (September to November), and (d) across all seasons. Error bars show one standard deviation.

ratio (max/min) of mass concentration values were higher than those of surface area concentration at all times, i.e., the diurnal variation of mass concentration was greater than that of surface area concentration in every season. A weak correlation ($R^2 = 0.31$) between $PM_{2.5}$ mass and surface area concentrations is shown in Fig. 4. This weak correlation likely results from temporal variation of particle size distribution of ambient aerosols. In other words, changes in the number of relatively larger particles affect the mass concentration of $PM_{2.5}$ whereas it does not affect the surface area concentration very much.

The mass concentration, surface area concentration and specific surface area of $PM_{2.5}$ in each season are shown in Table 2. The mean value of $PM_{2.5}$ specific surface area across all seasons is 10.3 ± 4.0 m^2/g. This specific surface area value is consistent with an estimated specific surface area value (11.9 m^2/g) for the fine particles whose mass-based particle size peak is 0.5 μm (Okuda, 2013). Compared with the BET method, the calculation method used in this study may have much larger uncertainty because this calculation involves uncertainties derived from the two measurement results, the DC method for surface area and the

Table 2. Mean values of surface area concentration, mass concentration and specific surface area of $PM_{2.5}$ in the 24-hour continuous measurements in each season of 2014.

Seasons	Surface area ($\mu m^2/cm^3$)	Mass ($\mu g/m^3$)	Specific surface area (m^2/g)	Samples
Spring (March to May)	119 ± 40	16.0 ± 5.1	7.5 ± 1.4	12
Summer (June to August)	135 ± 51	15.6 ± 10.7	10.2 ± 3.9	13
Fall (September to November)	160 ± 65	12.9 ± 4.8	12.9 ± 3.9	14
All seasons	139 ± 55	14.7 ± 7.3	10.3 ± 4.0	39

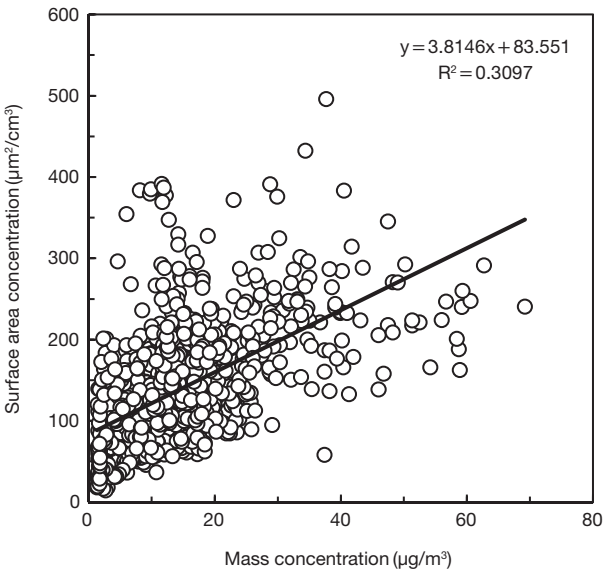

Fig. 4. Comparison between $PM_{2.5}$ mass concentration and surface area concentration in 24-hour continuous measurements. The measurements were carried out from March to November, 2014.

SHARP for $PM_{2.5}$. Nevertheless, the DC method for the determination of specific surface area has a much higher time resolution and simpler experimental handling compared with the BET method.

Fig. 5 shows the diurnal variation of $PM_{2.5}$ specific surface area in each season: (a) spring, (b) summer, (c) fall, and (d) all seasons. The specific surface area tends to decline during the daytime in each season. As shown in Figs. 2 and 3, the mass and surface area concentrations increase during the daytime in most cases; however, the variation in mass concentration is greater than that of surface area concentration. Therefore, specific surface area decreases during the daytime. Consequently, the abundance of relatively larger particles in $PM_{2.5}$ is considered to increase during the daytime through the measurement campaigns. This kind of diurnal variation of the ambient aerosol particle size distribution has been reported by other researchers (Yue *et al*., 2013; Sasaki and Sakamoto, 2006).

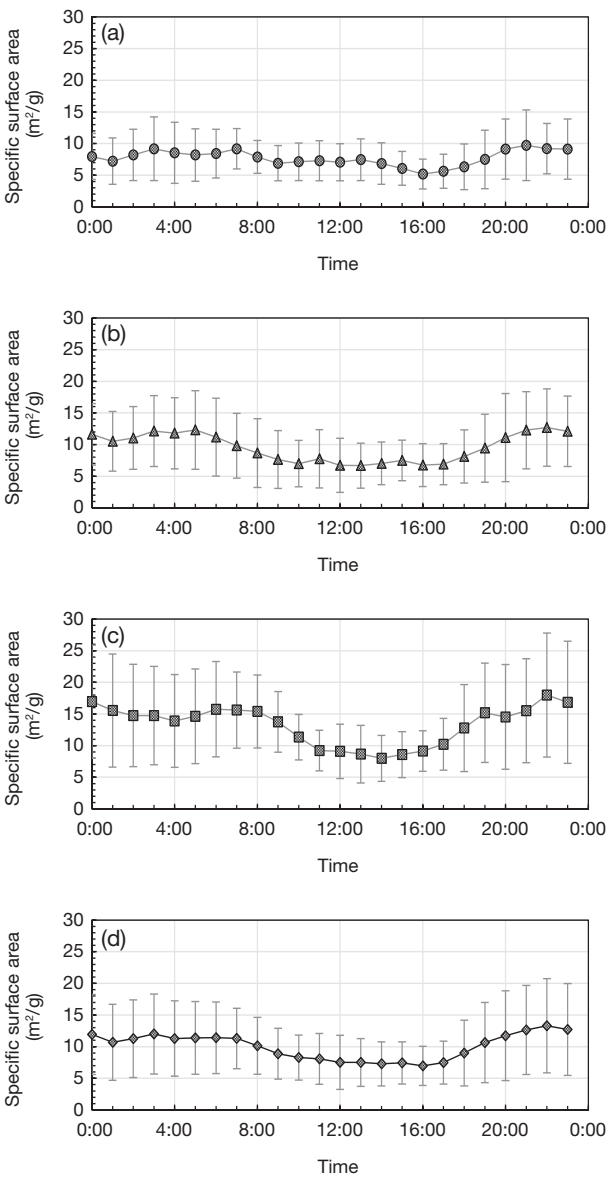

Fig. 5. Diurnal variation of $PM_{2.5}$ specific surface area measured using the NSAM and SHARP combined in 24-hour continuous measurements conducted in 2014. (a) Hourly mean values in spring (March to May), (b) summer (June to August), (c) fall (September to November), and (d) across all seasons. Error bars show one standard deviation.

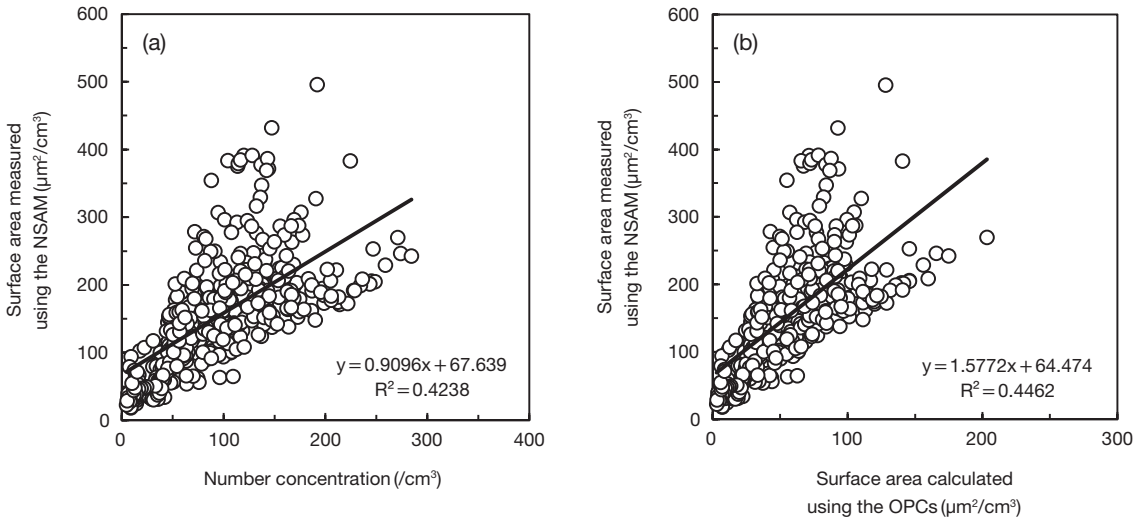

Fig. 6. Comparisons between $PM_{2.5}$ surface area concentration measured using the NSAM and $PM_{2.5}$ number and surface area concentrations measured using the OPC in 24-hour continuous measurements: (a) number concentration measured using the OPC and (b) surface area concentration calculated using the number concentration of the OPC. The measurements were carried out from July to November, 2014.

3. 2 Comparison between Surface Area and Number Concentration

In Fig. 6, the concentration of surface area of $PM_{2.5}$, measured using the NSAM, is compared with (a) the number concentration measured using the OPC that can measure the particles larger than 0.3 μm, and (b) the surface area concentration calculated using the OPCs, based on the assumption that the shape of particles is spherical and measured optical equivalent diameter is considered as geometric diameter ($=\pi \times D_p^2$). In this study, the diameter D_p for each channel of OPC was the geometric mean, the square root of upper × lower diameters (0.387, 0.707, 1.414, 3.162, and 7.071 μm). The coefficients of determination (R^2) were (a) 0.42 and (b) 0.45. It means that these correlations were not strong, and the conversion of number concentrations to calculated values of surface area concentrations did not improve the correlation with surface area concentration values measured using the NSAM. By taking closer look at Fig. 6b, it seems that there are two or more groups that have different slopes between NSAM surface area and OPC derived surface area. It means that sometimes the NSAM surface area can be explained mainly using the number of particles larger than 0.3 μm, but in many cases much smaller particles contributes mainly to the NSAM surface area. Ntziachristos *et al*. (2007b) measured the surface area concentration of ambient aerosols using the NSAM and measured number concentration using SMPS and a condensation particle counter (CPC). A linear regression between surface area concentrations measured with the NSAM and those calculated using the SMPS results at the two urban sites yielded much higher coefficients of determination of 0.94 and 0.64. Furthermore, reconstructed surface area using SMPS and CPC results gave much better approximation of the surface area measured by NSAM, thereby the reconstructed surface area to NSAM surface area ratios ranged from

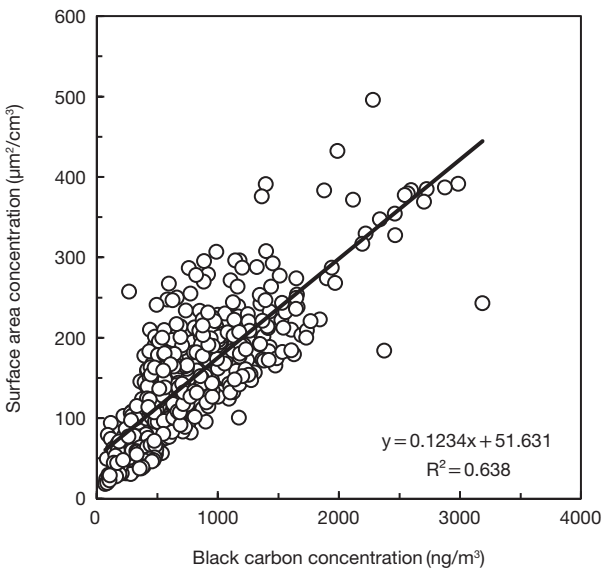

Fig. 7. Comparison between black carbon concentration and $PM_{2.5}$ surface area concentration in 24-hour continuous measurements. The measurements were carried out from June to November, 2014.

Table 3. Linear regressions between black carbon concentration and $PM_{2.5}$ surface area concentration in each 24-hour continuous measurement conducted in 2014. $PM_{2.5}$ concentrations, temperature and relative humidity for each sampling campaign were also shown. Meteorological data were obtained from JMA (2015).

No.	Sampling periods	Slope	Intercept	Coefficient of determination	$PM_{2.5}$ conc. ($\mu g/m^3$)	Temperature (°C)	Relative humidity (%)
1	06/19 18:00 - 06/20 18:00	0.15	24	0.39	9.7 ± 5.6	25.5 ± 2.2	59.5 ± 9.2
2	06/23 11:00 - 06/24 11:00	0.16	27	0.76	13.7 ± 7.0	24.8 ± 1.7	70.1 ± 11.5
3	06/24 14:00 - 06/25 14:00	−0.02	174	0.02	12.6 ± 4.6	22.0 ± 2.0	89.3 ± 11.0
4	06/25 16:00 - 06/26 16:00	0.09	60	0.30	14.1 ± 7.0	23.2 ± 2.2	77.3 ± 8.5
5	06/30 13:00 - 07/01 13:00	0.18	38	0.18	9.8 ± 3.4	24.1 ± 1.4	78.0 ± 8.7
6	07/31 14:00 - 08/01 14:00	0.14	25	0.83	11.5 ± 10.2	29.7 ± 2.0	70.0 ± 8.8
7	08/01 21:00 - 08/02 21:00	0.18	23	0.71	13.6 ± 11.3	30.3 ± 2.2	65.3 ± 9.4
8	08/03 08:00 - 08/04 08:00	0.21	24	0.83	9.0 ± 10.2	30.8 ± 2.0	62.9 ± 7.8
9	09/19 19:00 - 09/20 19:00	0.12	18	0.78	8.3 ± 2.3	21.0 ± 1.0	57.6 ± 4.5
10	09/20 19:00 - 09/21 19:00	0.05	96	0.07	11.8 ± 6.9	20.2 ± 2.6	61.2 ± 12.5
11	09/21 19:00 - 09/22 19:00	0.14	88	0.65	15.8 ± 10.7	21.9 ± 1.9	61.8 ± 10.2
12	10/17 15:00 - 10/18 15:00	0.20	−12	0.56	7.1 ± 7.2	16.5 ± 2.1	40.3 ± 5.2
13	10/18 15:00 - 10/19 15:00	0.11	106	0.42	18.1 ± 7.8	16.9 ± 2.2	60.5 ± 7.9
14	10/19 15:00 - 10/20 15:00	0.12	104	0.44	17.9 ± 5.5	18.6 ± 2.1	66.8 ± 8.3
15	10/25 18:00 - 10/26 18:00	0.08	140	0.40	19.1 ± 4.4	18.9 ± 1.9	80.7 ± 5.8
16	10/26 18:00 - 10/27 18:00	0.21	47	0.46	11.9 ± 2.5	19.8 ± 1.5	84.5 ± 11.7
17	11/05 20:00 - 11/06 20:00	0.14	26	0.84	15.5 ± 2.6	16.6 ± 1.6	76.7 ± 9.4
18	11/20 14:00 - 11/21 14:00	0.09	44	0.94	15.5 ± 3.1	8.8 ± 1.6	91.0 ± 10.7
19	11/21 14:00 - 11/22 14:00	0.09	96	0.83	16.7 ± 5.5	11.8 ± 1.8	82.5 ± 9.8
20	11/25 14:00 - 11/26 14:00	0.07	19	0.97	6.7 ± 5.6	9.3 ± 1.1	98.5 ± 1.6
21	11/26 14:00 - 11/27 14:00	0.16	2	0.93	3.8 ± 3.5	9.8 ± 1.5	93.0 ± 10.1
22	11/27 14:00 - 11/28 14:00	0.09	127	0.88	12.4 ± 3.7	12.5 ± 1.2	83.9 ± 9.1

0.71 to 0.90. These findings suggest that the $PM_{2.5}$ surface area concentration is mainly governed by the abundance of much smaller particles whose diameter is less than 0.3 μm.

3. 3 Comparison between Surface Area and Black Carbon Concentrations

The concentrations of the surface area of $PM_{2.5}$ and BC were measured continuously for 24 hours from June to November, 2014 (Fig. 7). These concentrations were highly correlated ($R^2 = 0.64$). Therefore, the abundance of BC particles is considered to affect the total surface area concentration of $PM_{2.5}$ because of the smaller primary particles of BC. Table 3 shows the linear regression results for each measurement, along with $PM_{2.5}$ mass concentration measured by SHARP, ambient temperature, and relative humidity (JMA, 2015). The maximum coefficient of determination is 0.97 (No. 20) and the minimum is 0.02 (No. 3). This indicates that the strength of the correlation varied considerably among the experiments. Coefficient of determination of surface area with BC did not show clear correlations with $PM_{2.5}$ mass concentration, ambient temperature, or relative humidity. Air mass backward trajectories calculated for each measurement campaign using NOAA HYSPLIT model (Draxler and Rolph, 2015; Rolph, 2015); however, the air mass origin and trajectories did not seem to affect the correlation between surface area and BC.

Fig. 8 shows how the correlation between surface area and BC concentrations differs over time: (a) night (0:00 to 6:00), (b) morning (6:00 to 12:00), (c) afternoon (12:00 to 18:00), and (d) evening (18:00 to 24:00). The coefficients of determination were (a) 0.81, (b) 0.66, (c) 0.42, and (d) 0.76, which indicate a relatively weaker afternoon correlation compared with the other three time zones. It is possible that the particles other than BC that affects surface area concentration may be transported and/or secondarily formed during the daytime. This idea is also supported by the findings that the abundance of relatively larger particles in $PM_{2.5}$ is considered to increase during the daytime during the measurement campaigns as mentioned above.

The weak afternoon correlation can also be attributed to variation in the mixing state and morphology of the BC particles (China *et al*., 2014). In general, some of the BC particles in the ambient air are considered to be coated with organic carbon (OC: China *et al*., 2014; China *et al*., 2013). If these particles are heavily coated with OC, their specific surface area is likely to decrease significantly. Moreover, Moteki *et al*. (2014) showed that the abundance of coated BC particles among total

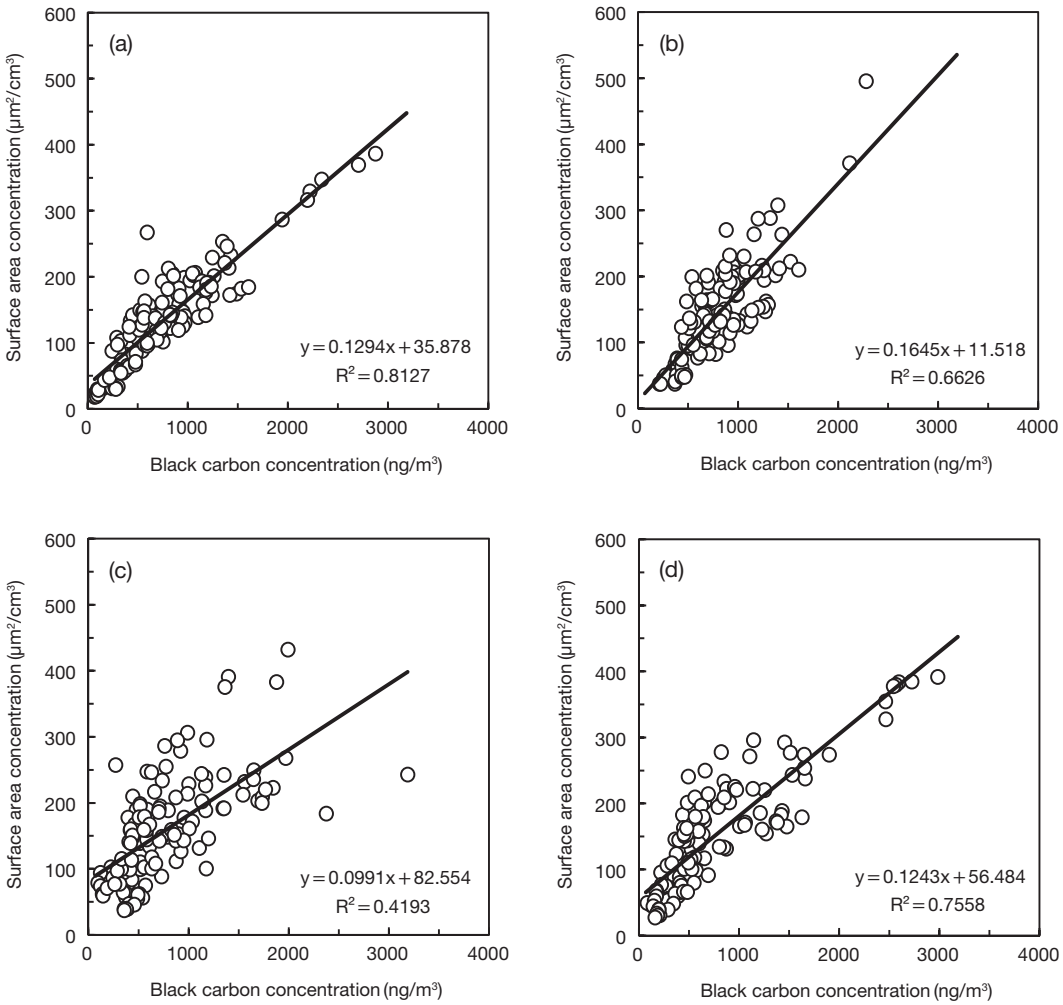

Fig. 8. Comparisons of correlations between black carbon concentration and $PM_{2.5}$ surface area concentrations in four time zones: (a) night (0:00 to 6:00), (b) morning (6:00 to 12:00), (c) afternoon (12:00 to 18:00), and (d) evening (18:00 to 0:00), using the data presented in Fig. 7.

BC-containing particles can vary considerably with time. In addition, the abundance of coated BC particles varies with emission sources (China *et al*., 2014; China *et al*., 2013). Therefore, it is conceivable that the strength of the correlation declines if the abundance of coated BC particles increases in the afternoon.

Polidori *et al*. (2008) compared surface area concentrations measured using the NSAM and BC concentrations measured using an aethalometer at a sampling site located near major freeways. They found that the strength of the correlation between surface area and BC concentrations did not change considerably across four time zones similar to those used in this study (R^2 = 0.67-0.82). We believe that this is due to the consistently high abundance of bare BC particles (i.e., not coated with OC) freshly emitted from automotive vehicles near freeways (China *et al*., 2014), and thus the specific surface area of the BC particles was high at all times. Consequently, the strength of the correlation between BC concentration and total surface area concentration of ambient aerosols are likely to vary according to sampling environment.

In Fig. 9, the BC concentration is compared with four different concentrations of $PM_{2.5}$: (a) number concentration measured using the OPC, (b) surface area concentration measured using the NSAM, (c) surface area concentration calculated from the OPC number concentration, and (d) mass concentration measured using the SHARP. The coefficients of determination are (a) 0.40, (b) 0.64, (c) 0.41, and (d) 0.12, which indicate that the BC concentration correlates best with $PM_{2.5}$ surface area concentration measured using the NSAM.

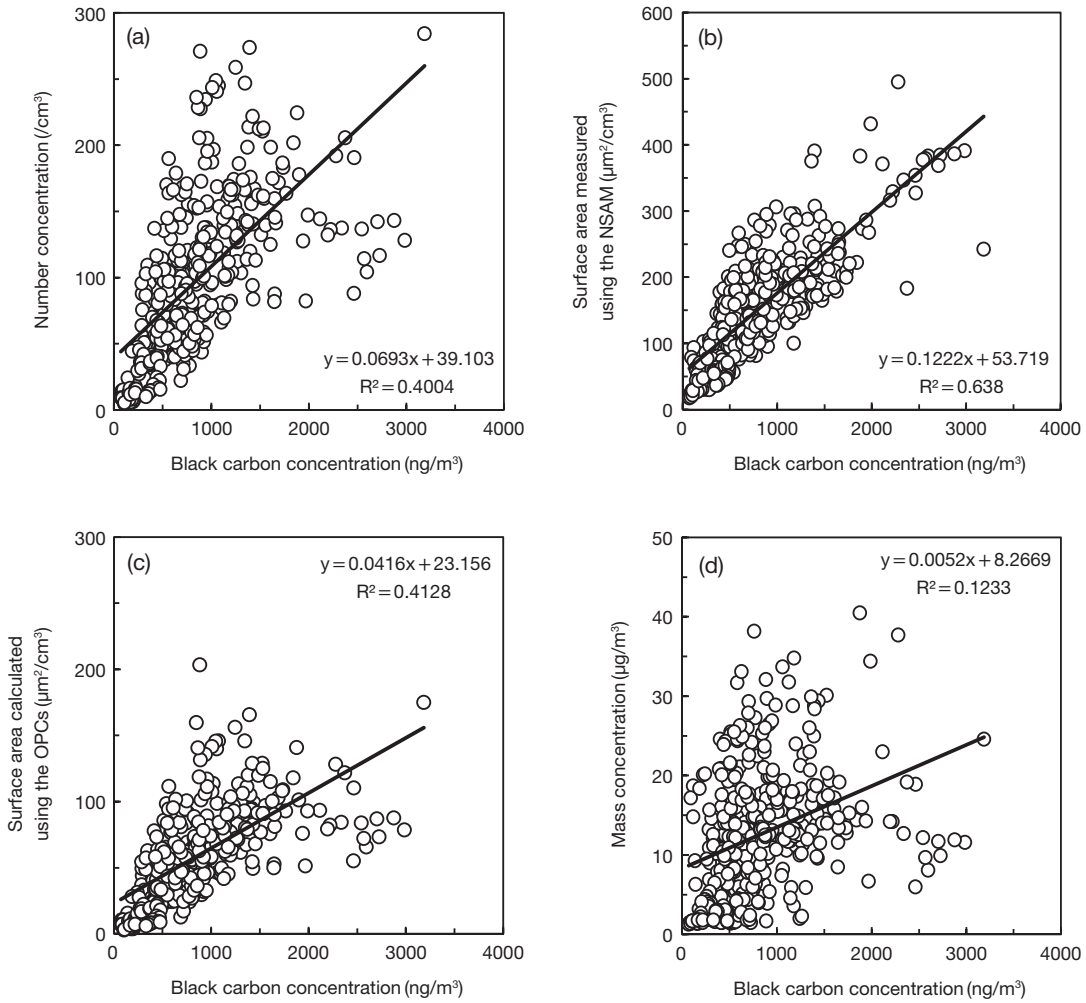

Fig. 9. Comparisons between black carbon concentration and four different $PM_{2.5}$ concentrations in 24-hour continuous measurements: (a) number concentration measured using the OPC (>0.3 μm); (b) surface area concentration measured using the NSAM; (c) surface area concentration calculated using the OPC number concentration; and (d) mass concentration measured using the SHARP. The measurements were carried out from July to November, 2014.

4. CONCLUSION

The surface area concentration of $PM_{2.5}$ was measured in this study using the DC method. In addition, the mass and number concentrations of $PM_{2.5}$ and the BC concentration were measured simultaneously, and the way in which these three concentrations affected the surface area concentration was investigated. The 24-hour continuous measurement campaigns were carried out 39 times from March to November, 2014 in Yokohama, Japan. A comparison between the mass concentration and surface area concentration of $PM_{2.5}$ did not show a clear 1:1 correspondence. Hence, measurements of the $PM_{2.5}$ surface area concentration are needed in addition to measurements of the $PM_{2.5}$ mass concentration, which are already carried out extensively by research institutions and administrative organizations, for a more detailed evaluation of the adverse health effects caused by $PM_{2.5}$.

The surface area concentration of $PM_{2.5}$ was more closely correlated to the BC concentration than the mass concentration of $PM_{2.5}$. This indicates that the abundance of BC particles significantly affects the surface area concentration of $PM_{2.5}$. The strength of the correlation between surface area and BC varied considerably among the measurement campaigns. We consider that this is due to the transportation/formation of the particles other than BC that affects surface area concentration and/or the variation of the surface condition of the BC particles.

ACKNOWLEDGEMENT

This study was supported partly by JSPS/MEXT KAKENHI Grant Number 26340010, Steel Foundation for Environmental Protection Technology, Grant for Environmental Research Projects from The Sumitomo Foundation, and Keio Gijuku Academic Development Funds.

REFERENCES

Albuquerque, P.C., Gomes, J.F., Bordado, J.C. (2012) Assessment of exposure to airborne ultrafine particles in the urban environment of Lisbon, Portugal. Journal of the Air & Waste Management Association 62, 373-380.

Asbach, C., Fissan, H., Stahlmecke, B., Kuhlbusch, T.A.J., Pui, D.Y.H. (2009) Conceptual limitations and extensions of lung-deposited Nanoparticle Surface Area Monitor (NSAM). Journal of Nanoparticle Research 11, 101-109.

Bau, S., Witschger, O., Gensdarmes, F., Rastoix, O., Thomas, D. (2010) A TEM-based method as an alternative to the BET method for measuring off-line the specific surface area of nanoaerosols. Powder Technology 200, 190-201

Bau, S., Witschger, O., Gensdarmes, F., Thomas, D. (2012) Evaluating three direct-reading instruments based on diffusion charging to measure surface area concentrations in polydisperse nanoaerosols in molecular and transition regimes. Journal of Nanoparticle Research 14, 1217.

Brunauer, S., Emmett, P.H., Teller, E. (1938) Adsorption of gases in multimolecular layers. Journal of American Chemical Society 60, 309-319.

Cai, J., Yan, B., Ross, J., Zhang, D., Kinney, P.L., Perzanowski, M.S., Jung, K.H., Miller, R., Chillrud, S.N. (2014) Validation of microAeth® as a black carbon monitor for fixed-site measurement and optimization for personal exposure characterization. Aerosol and Air Quality Research 14, 1-9.

Cheng, Y.H., Lin, M.H. (2013) Real-time performance of the microAeth® AE51 and the effects of aerosol loading on its measurement results at a traffic site. Aerosol and Air Quality Research 13, 1853-1863.

China, S., Mazzoleni, C., Gorkowski, K., Aiken, A.C., Dubey, M.K. (2013) Morphology and mixing state of individual freshly emitted wildfire carbonaceous particles. Nature Communications 4, 2122.

China, S., Salvadori, N., Mazzoleni, C. (2014) Effect of traffic and driving characteristics on morphology of atmospheric soot particles at freeway on-ramps. Environmental Science & Technology 48, 3128-3135.

Donaldson, K., Li, X.Y., MacNee, W. (1998) Ultrafine (nanometre) particle mediated lung injury. Journal of Aerosol Science 29, 553-560.

Draxler, R.R., Rolph, G.D. (2015) HYSPLIT (HYbrid Single-Particle Lagrangian Integrated Trajectory) Model access via NOAA ARL READY Website (http://ready.arl.noaa.gov/HYSPLIT.php). NOAA Air Resources Laboratory, Silver Spring, MD.

Ferrero, L., Mocnik, G., Ferrini, B.S., Perrone, M.G., Sangiorgi, G., Bolzacchini, E. (2011) Vertical profiles of aerosol absorption coefficient from micro-Aethalometer data and Mie calculation over Milan. Science of the Total Environment 409, 2824-2837.

Fissan, H., Neumann, S., Trampe, A., Pui, D.Y.H., Shin, W.G. (2007) Rationale and principle of an instrument measuring lung deposited nanoparticle surface area. Journal of Nanoparticle Research 9, 53-59.

Gäggeler, H.W., Baltensperger, U., Emmenegger, M., Jost, D.T., Schmidt-Ott, A., Haller, P., Hofmann, M. (1989) The epiphaniometer, a new device for continuous aerosol monitoring. Journal of Aerosol Science 20, 557-564.

Giechaskiel, B., Alföldy, B., Drossinos, Y. (2009) A metric for health effects studies of diesel exhaust particles. Journal of Aerosol Science 40, 639-651.

Heitbrink, W.A., Evans, D.E., Ku, B.K., Maynard, A.D., Slavin, T.J., Peters, T.M. (2009) Relationships among particle number, surface area, and respirable mass concentrations in automotive engine manufacturing. Journal of Occupational and Environmental Hygiene 6, 19-31.

International Commission on Radiological Protection (1994) Human respiratory tract model for radiological protection. ICRP Publication 66. Annals of the ICRP 24 (1-3):1-482

Japan Meteorological Agency (2015) Meteorological Data Archives. http://www.data.jma.go.jp/obd/stats/etrn/index.php (in Japanese)

Jung, H., Kittelson, D.B. (2005) Characterization of aerosol surface instruments in transition regime. Aerosol Science and Technology 39, 902-911.

Kaminski, H., Kuhlbusch, T.A.J., Rath, S., Götz, U., Sprenger, M., Wels, D., Polloczek, J., Bachmann, V., Dziurowitz, N., Kiesling, H.-J., Schwiegelshohn, A., Monz, C., Dahmann, D., Asbach, C. (2013) Comparability of mobility particle sizers and diffusion chargers, Journal of Aerosol Science 57, 156-178.

Kittelson, D.B., Watts, W.F., Savstrom, J.C., Johnson, J.P. (2005) Influence of a catalytic stripper on the response of real time aerosol instruments to diesel exhaust aerosol. Journal of Aerosol Science 36, 1089-1107.

Ku, B.K. (2010) Determination of the ratio of diffusion charging-based surface area to geometric surface area for spherical particles in the size range of 100-900 nm. Journal of Aerosol Science 41, 835-847.

Kulkarni, P., Baron, P.A., Willeke, K. (2011) Aerosol Measurement: Principles, Techniques, and Applications, 3rd Edition. John Wiley & Sons, Inc., New Jersey.

Leavey, A., Fang, J., Sahu, M., Biswas, P. (2013) Comparison of measured particle lung-deposited surface area concentrations by an Aerotrak 9000 using size distribution measurements for a range of combustion aero-

sols, Aerosol Science and Technology 47, 966-978.
LeBouf, R.F., Ku, B.K., Chen, B.T., Frazer, D.G., Cumpston, J.L., Stefaniak, A.B. (2011) Measuring surface area of airborne titanium dioxide powder agglomerates: relationships between gas adsorption, diffusion and mobility-based methods. Journal of Nanoparticle Research 13, 7029-7039.
Mokhtar, M.-A., Jayaratne, R., Morawska, L., Mazaheri, M., Surawski, N., Buonanno, G. (2013) NSAM-derived total surface area versus SMPS-derived "mobility equivalent" surface area for different environmentally relevant aerosols. Journal of Aerosol Science 66, 1-11.
Moteki, N., Kondo, Y., Adachi, K. (2014) Identification by single-particle soot photometer of black carbon particles attached to other particles: Laboratory experiments and ground observations in Tokyo. Journal of Geophysical Research-Atmospheres 119, 1031-1043.
Nakanishi, J. (2011) Risk Assessment of Manufactured Nanomaterials "Approaches" - Overview of Approaches and Results - Final Report issued on August 17, 2011 Revised on February 22, 2013 NEDO Project (P06041) "Research and Development of Nanoparticle Characterization Methods."
Nguyen, T.H., Ball, W.P. (2006) Absorption and adsorption of hydrophobic organic contaminants to diesel and hexane soot. Environmental Science & Technology 40, 2958-2964.
Ntziachristos, L., Giechaskiel, B., Ristimäki, J., Keskinen, J. (2004) Use of a corona charger for the characterisation of automotive exhaust aerosol. Journal of Aerosol Science 35, 943-963.
Ntziachristos, L., Ning, Z., Geller, M.D., Sioutas, C. (2007a) Particle concentration and characteristics near a major freeway with heavy-duty diesel traffic. Environmental Science & Technology 41, 2223-2230.
Ntziachristos, L., Polidori, A., Phuleria, H., Geller, M.D., Sioutas, C. (2007b) Application of a diffusion charger for the measurement of particle surface concentration in different environments. Aerosol Science and Technology 41, 571-580.
Oberdörster, G. (2001) Pulmonary effects of inhaled ultrafine particles. International Archives of Occupational and Environmental Health 74, 1-8.
Oberdörster, G., Finkelstein, J.N., Johnston, C., Gelein, R., Cox, C., Baggs, R., Elder, A.C.P. (2000) Acute pulmonary effects of ultrafine particles in rats and mice. Research Report Health Effects Institute 96, 5-74.
Oberdörster, G., Gelein, R.M., Ferin, J., Weiss, B. (1995) Association of particulate air pollution and acute mortality: involvement of ultrafine particles?. Inhalation Toxicology 7, 111-124.
Oberdörster, G., Oberdörster, E., Oberdörster, J. (2005) Nanotoxicology: An emerging discipline evolving from studies of ultrafine particles. Environmental Health Perspectives 113, 823-839.
Okuda, T. (2013) Measurement of the specific surface area and particle size distribution of atmospheric aerosol reference materials. Atmospheric Environment 75, 1-5.
Okuda, T., Isobe, R., Nagai, Y., Okahisa, S., Funato, K., Inoue, K. (2015) Development of a high-volume $PM_{2.5}$ particle sampler using impactor and cyclone techniques. Aerosol and Air Quality Research 15, 759-767.
Okuda, T., Nakao, S., Katsuno, M., Tanaka, S. (2007) Source identification of nickel in TSP and $PM_{2.5}$ in Tokyo, Japan, Atmospheric Environment 41, 7642-7648.
Polidori, A., Hu, S., Biswas, S., Delfino, R.J., Sioutas, C. (2008) Real-time characterization of particle-bound polycyclic aromatic hydrocarbons in ambient aerosols and from motor-vehicle exhaust. Atmospheric Chemistry and Physics 8, 1277-1291.
Rolph, G.D. (2015) Real-time Environmental Applications and Display sYstem (READY) Website (http://ready.arl.noaa.gov). NOAA Air Resources Laboratory, Silver Spring, MD.
Rule, A.M., Geyh, A.S., Ramos-Bonilla, J.P., Mihalic, J.N., Margulies, J.D., Polyak, L.M., Kesavan, J., Breysse, P.N. (2010) Design and characterization of a sequential cyclone system for the collection of bulk particulate matter. Journal of Environmental Monitoring 12, 1807-1814.
Sasaki, K., Sakamoto, K. (2006) Diurnal characteristics of suspended particulate matter and $PM_{2.5}$ in the urban and suburban atmosphere of the Kanto Plain, Japan. Water, Air, & Soil Pollution 171, 29-47.
Shin, W.G., Pui, D.Y.H., Fissan, H., Neumann, S., Trampe, A. (2007) Calibration and numerical simulation of Nanoparticle Surface Area Monitor (TSI Model 3550 NSAM). Journal of Nanoparticle Research 9, 61-69.
TSI Incorporated (2010) Measuring Nanoparticle Exposure, Application Note NSAM-001.
United States Environmental Protection Agency (2009) Federal Register / Vol. 74, No. 104 / Tuesday, June 2, 2009 / Notices.
Vincent, J.H. (ed) (1999) Particle size-selective sampling for particulate air contaminants. American Conference for Governmental Industrial Hygienists (ACGIH), Cincinnati, OH.
Velasco, E., Siegmann, P., Siegmann, H.C. (2004) Exploratory study of particle-bound polycyclic aromatic hydrocarbons in different environments of Mexico City. Atmospheric Environment 38, 4957-4968.
Whitby, K.T. (1978) The physical characteristics of sulfur aerosols. Atmospheric Environment 12, 135-159.
World Health Organization (2005). WHO Air quality guidelines for particulate matter, ozone, nitrogen dioxide and sulfur dioxide Global update 2005 Summary of risk assessment. WHO press, Geneva.
Yue, D.L., Hu, M., Wang, Z.B., Wen, M.T., Guo, S., Zhong, L.J., Wiedensohler, A., Zhang, Y.H. (2013) Comparison of particle number size distributions and new particle formation between the urban and rural sites in the PRD region, China. Atmospheric Environment 76, 181-188.

(Received 28 October 2015, revised 18 December 2015, accepted 26 December 2015)